2020 IEEE/RSJ International Conference on Intelligent Robots and Systems (IROS)
October 25-29, 2020, Las Vegas, NV, USA (Virtual)

Impedance Control of Humanoid Walking on Uneven Terrain With Centroidal Momentum Dynamics Using Quadratic Programming

Joonhee Jo[1,2] and Yonghwan Oh[1]

Abstract— **In this paper, we propose the stabilization strategy for a soft landing in a biped walking using impedance control and the optimization-based whole-body control framework. Even though proper contact forces and desired trajectories of the robot are given, the robot can be unstable easily if unexpected forces are applied to the robot or impulsive contact force is produced in the landing state while the robot is walking. Therefore, the impedance control approach using contact forces is performed to obtain the modified references that regulate the modified desired position, velocity and acceleration of the swing foot, and improves the walking stability. Moreover, we perform a whole-body control using quadratic programming (QP) that tracks the modified trajectories constrained with the centroidal momentum dynamics. To validate the algorithm, a walking task on uneven terrain using a humanoid robot is shown.**

I. Introduction

Humanoid robot is designed to perform a variety of tasks including interaction in complex environments. A walking task is the basic interaction task with the ground/environment considering the contact forces. If the ground contact force is properly controlled, the balance control can be obtained. Throughout the research, the balancing control of humanoid robot is studied in a variety of ways such as the center of mass (CoM) tracking using inverse kinematics [1] with floating base [2], and inverse dynamics onto independent space of contact forces by using an orthogonal decomposition [3]. A model-based torque control approach is also performed to show compliant interaction [4].

These approaches have difficulties in considering unilateral contact forces from ground. To consider the unilateral contact forces, constrained optimization techniques with friction approximation are developed. This approximation is performed using quadratic programming (QP) that leads to finding joint torques with constrained ground contact force and given tasks [5]–[7]. In addition to this, centroidal momentum based control with QP is also studied [8]–[10]. This paper used centroidal momentum dynamics to resolve the acceleration of the generalized coordinates and ground contact forces with the friction approximation by using QP while the tasks are tracked.

In addition, the walking trajectory generation has been studied while having balance control to improve the stability of the robot. For decades, CoM trajectory generation algorithms are introduced with linear inverted pendulum mode (LIPM) [11]. The conventional trajectory generation using LIPM is not robust to unexpected external forces. Hence, online trajectory optimization algorithms have been researched [12], [13]. These methods consider the modification of the robot's step location. However, if there is unexpected contact force from the ground, it produces instability of the robot walking because it disturbs the swing leg's landing if there is no additional feedback such as vision sensor feedback. Hence, soft landing control of the walking robot should also be considered in the landing state.

Unexpected contact force at the foot occurs when a robot walks on an uneven terrain which changes the height or altitude of the terrain. To resolve the problem, some researches proposed real-time walking state adjustment strategy using slope mode judgment [14], virtual spring-damper to absorb the shock at landing between the hip joint and ankle joint [15], and at ankle [16], at foot [17]. Some research used time-domain passivity methods to reduce the z-axis impact energy [18], with tiled posture of robot at pitch axis [19]. Those algorithms presented the landing force reduction by passivity control. On the other hand, impedance control based landing control is researched to obtain the reference trajectory for the computed torque method [20]. In addition, position modification is obtained in [21] and roll-pitch motion at ankle [22].

The landing task is defined as 1) maintain the position at contact, 2) regulate the velocity as fast. When the foot comes to contact, uneven terrain yields the unexpected landing in the z-axis of position and x-axis & y-axis orientation most. To regulate the velocity of the landing foot in three axes, the impedance control based reference trajectory modification algorithm is applied in this paper. The algorithm works at the swing phase because the stance foot is assumed to be having zero acceleration.

The walking trajectory is given from LIPM that generates CoM-ZMP trajectories [23]. During the walk, if the robot has steps on irregular ground, the impedance controller modifies the walking trajectory, velocity, and acceleration to adapt the unexpected landing, and generates modified reference acceleration to apply to the QP framework as input.

This paper proposes soft landing control with impedance control based reference modification in section II and derives the equation of motion of the biped robot with contact constraints in section III for tracking and balancing control. In addition, the optimal contact force is obtained from QP with inequality/equality constraints and control input is formed with reference tasks. Using the proposed control framework, the simulation is performed to establish the improved performance and results of an experiment are

[1]J. Jo and Y. Oh are with Center for Intelligent & Interactive Robotics, Korea Institute of Science and Technology (KIST), Seoul, 136-791, Korea (email: jhjo@kist.re.kr and oyh@kist.re.kr)

[2]Department of HCI & Robotics, University of Science and Technology(UST), Daejeon, 305-350, Korea

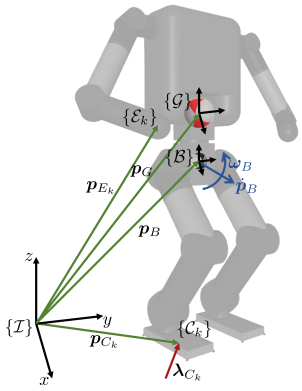

Fig. 1. A humanoid robot. n joints are equipped in active joints, and 6 passive joints in the body. Each contacts on the ground are considered as frictional point contact. $\{\mathcal{B}\}$ is the body frame, $\{\mathcal{G}\}$ is the center of mass(CoM) frame, $\{\mathcal{E}_k\}$ is End-effector frame, $\{\mathcal{C}_k\}$ is the contact frame, $\{\mathcal{I}\}$ inertial frame.

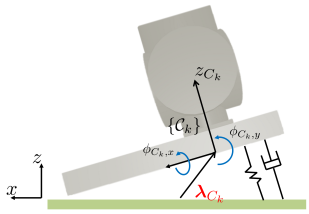

Fig. 2. Foot system modelling for the impedance control. The force from the ground to the foot is the input and the position/angle are the output.

discussed in section IV. Finally, concluding remarks are in section V.

II. Compensation Using Impedance Control

During the walk, it is assumed that the walking trajectory is given, and the legs travel from the stance to swing state according to the given trajectory. The robot controller needs proper control gains to keep tracking the given trajectories. Higher proportional control gains can cause of instability at the contact moment. In addition, lower proportional control gains can cause insufficient tracking performance and it also can cause the break of the stability. In the case of damping gain, overdamping can cause oscillations so it has limit to be increased. Hence, two approaches to overcome can be considered : 1) to lower the proportional gains and higher the damping gains at the moment of contact, 2) to modify the desired trajectory to adapt the unexpected landing. This paper is based on the second approach using impedance control using F/T sensors mounted between the foot and ankle. The impedance control enhances in reduction of the impact force by unexpected landing and regulation of velocity in swing phase.

The desired impedance of the foot system described in Fig. 2 is

$$\begin{aligned}\boldsymbol{M}_d\left(\ddot{\boldsymbol{x}}_{C_k}-\ddot{\boldsymbol{x}}_{C_k,d}\right)+\boldsymbol{B}_d\left(\dot{\boldsymbol{x}}_{C_k}-\dot{\boldsymbol{x}}_{C_k,d}\right)\\ +\boldsymbol{K}_d\left(\boldsymbol{x}_{C_k}-\boldsymbol{x}_{C_k,d}\right)=\boldsymbol{\lambda}_{C_k}.\end{aligned} \tag{1}$$

where $\boldsymbol{M}_d, \boldsymbol{B}_d, \boldsymbol{K}_d$ are the desired mass, damping, and stiffness gain. $\boldsymbol{x}_{C_k} = \begin{bmatrix}0\ 0\ z_{C_k}\ \phi_{C_k,x}\ \phi_{C_k,y}\ 0\end{bmatrix}^T$ and $\boldsymbol{\lambda}_{C_k}$ is the contact force. The reference acceleration satisfying the desired impedance of (1) can be obtained and it becomes modified acceleration

$$\ddot{\boldsymbol{x}}_{C_k,m} = \ddot{\boldsymbol{x}}_{C_k,d} + \boldsymbol{M}_d^{-1}\left(\boldsymbol{\lambda}_{C_k} + \boldsymbol{B}_d\dot{\boldsymbol{e}}_{C_k} + \boldsymbol{K}_d\boldsymbol{e}_{C_k}\right) \tag{2}$$

where $\boldsymbol{e}_{C_k} = \boldsymbol{x}_{C_k,d} - \boldsymbol{x}_{C_k}$. Modified velocity $\dot{\boldsymbol{x}}_{E_k,m}$ and modified position $\boldsymbol{x}_{E_k,m}$ can be achieved by numerical integration. In addition, the modified trajectories satisfy the impedance behavior. Hence, new reference acceleration for the foot at the contact moment can be defined

$$\ddot{\boldsymbol{x}}_{C_k,r} = \ddot{\boldsymbol{x}}_{C_k,m} + \boldsymbol{K}_v\left(\dot{\boldsymbol{x}}_{C_k,m} - \dot{\boldsymbol{x}}_{C_k}\right) + \boldsymbol{K}_p\left(\boldsymbol{x}_{C_k,m} - \boldsymbol{x}_{C_k}\right) \tag{3}$$

and modified reference acceleration is based on the impedance control to adapt the unexpected contact especially in the case of early contact and used in the QP framework. If there is no contact at foot, originally planned reference trajectory will be input. In addition, if there is unexpected contact at foot during swing phase, the modified reference induced by $\boldsymbol{\lambda}_{C_k}$ will be input.

III. Robot Modelling and Problem Formulation

For a humanoid robot which has $n+6$ degrees of freedom (DoF) including a floating body with 6 DoF and legs with n DoF, generalized coordinates velocity is defined as

$$\dot{\boldsymbol{\xi}}_B = \begin{bmatrix}\dot{\boldsymbol{p}}_B\\ \boldsymbol{\omega}_B\\ \dot{\boldsymbol{q}}\end{bmatrix} \in \Re^{n+6} \tag{4}$$

where $\dot{\boldsymbol{p}}_B, \boldsymbol{\omega}_B \in \Re^6$ are linear and angular velocities of the floating body and $\dot{\boldsymbol{q}} \in \Re^n$ is joint velocity.

A. A robot model

The equations of motion (EoM) of the robot system described in Fig. 1 are expressed as

$$\begin{aligned}&\underbrace{\begin{bmatrix}\boldsymbol{M}_B\\ \boldsymbol{M}_q\end{bmatrix}}_{\boldsymbol{M}}\ddot{\boldsymbol{\xi}} + \underbrace{\begin{bmatrix}\boldsymbol{C}_B\\ \boldsymbol{C}_q\end{bmatrix}}_{\boldsymbol{C}}\dot{\boldsymbol{\xi}} + \underbrace{\begin{bmatrix}\boldsymbol{g}_B\\ \boldsymbol{g}_q\end{bmatrix}}_{\boldsymbol{g}}\\ &= \underbrace{\begin{bmatrix}\boldsymbol{0}\\ \boldsymbol{B}_q\end{bmatrix}}_{\boldsymbol{B}}\boldsymbol{\tau} + \sum_k^{N_e}\underbrace{\begin{bmatrix}\boldsymbol{X}_{C_kB}^T\\ \hat{\boldsymbol{J}}_{C_k}^T\end{bmatrix}}_{\boldsymbol{X}_{C_k}^T}\boldsymbol{\lambda}_{C_k},\quad N_e = r,l\end{aligned} \tag{5}$$

$$\text{where}\quad \boldsymbol{X}_{C_kB} = \begin{bmatrix}\boldsymbol{E}_3 & \boldsymbol{0}\\ \$(\boldsymbol{p}_{C_kB}) & \boldsymbol{E}_3\end{bmatrix}$$

where $\boldsymbol{M}, \boldsymbol{C} \in \Re^{(n+6)\times(n+6)}$ are an inertia and a Coriolis and Centrifugal matrices of the body and $\boldsymbol{g} \in \Re^{(n+6)}$ is a gravitational force vector of the body. $\boldsymbol{B} \in \Re^{(n+6)\times n}$ is a selection matrix. $\boldsymbol{X}_{C_kB}, \hat{\boldsymbol{J}}_{C_k}$ are the part of Jacobian where the former is related to the body velocity and the latter is related to the joint velocity. $\$(*)$ is the skew-symmetric operator and $\boldsymbol{\lambda}_{C_k} = \begin{bmatrix}\boldsymbol{f}_C^T\ \boldsymbol{\mu}_C^T\end{bmatrix}^T \in \Re^k$ is the ground contact force vector. Joint torque $\boldsymbol{\tau}$ is dependent on joint acceleration $\ddot{\boldsymbol{q}}$ and $\boldsymbol{\lambda}_{C_k}$.

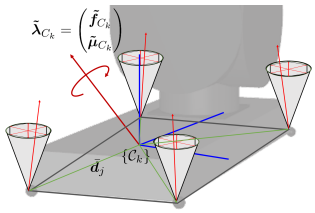

Fig. 3. Friction model used in quadratic programing formulation. It is unilateral contact in the frame $\{\mathcal{C}_k\}$.

B. Centroidal momentum dynamics

Total external force and moments applied to the $\{\mathcal{B}\}$ are related to the robot dynamics

$$\boldsymbol{\lambda}_B = \sum_k^{N_e} \boldsymbol{X}_{C_k B}^T \boldsymbol{\lambda}_{C_k} - \boldsymbol{g}_B = \boldsymbol{M}_B \ddot{\boldsymbol{\xi}} + \boldsymbol{C}_B \dot{\boldsymbol{\xi}}. \tag{6}$$

In addition, sum of external forces including ground contact force which are applied to the robot is equal to the rate of change of centroidal momentum,

$$\begin{aligned} \dot{\boldsymbol{h}}_G &= \boldsymbol{A}_G \ddot{\boldsymbol{\xi}} + \dot{\boldsymbol{A}}_G \dot{\boldsymbol{\xi}} = \boldsymbol{X}_{GB}^{-T} \boldsymbol{h}_B = \boldsymbol{X}_{GB}^{-T} (\boldsymbol{M}_B \ddot{\boldsymbol{\xi}} + \boldsymbol{C}_B \dot{\boldsymbol{\xi}}) \\ &= \boldsymbol{X}_{GB}^{-T} (\sum_k^{N_e} \boldsymbol{X}_{C_k B}^T \boldsymbol{\lambda}_{C_k} - \boldsymbol{g}_B). \end{aligned} \tag{7}$$

where $\dot{\boldsymbol{h}}_G$ is the centroidal momentum and $\dot{\boldsymbol{h}}_B$ is the body momentum. $\boldsymbol{A}_G, \dot{\boldsymbol{A}}_G$ is the centroidal momentum matrix and its derivative. $\boldsymbol{X}_{C_k G}$ is the adjoint transformation matrix from $\{\mathcal{G}\}$ to $\{\mathcal{C}_k\}$ and $\boldsymbol{X}_{GB}$ from $\{\mathcal{B}\}$ to $\{\mathcal{G}\}$. Additionally, $\boldsymbol{g}_G = m_G \begin{pmatrix} \bar{\boldsymbol{g}}^T & \boldsymbol{0}^T \end{pmatrix}^T$ and $\bar{\boldsymbol{g}}$ is the gravity vector.

Hence, rate of momentum change can be described using $\ddot{\boldsymbol{\xi}}$ and $\boldsymbol{\lambda}_{C_k}$. In this paper, centroidal momentum dynamics are transformed into body frame dynamics to reduce the computation. Since the equation of motion is derived w.r.t. $\{\mathcal{B}\}$, no more computation is necessary but just a transformation of centroidal momentum to body frame is required.

C. Friction cone approximation

In the right side of rate of change of momentum, ground contact forces are free variable to be decided by QP with constraints. The ground contact force is unilateral and modeled as frictional point contact with Coulomb friction. The Coulomb friction is the second order cone constraint which cannot be solved sufficiently fast with conventional solvers, and thus it is approximated by the m-dimensional polygon [24]

$$\tilde{\boldsymbol{\lambda}}_{C_k} = \begin{pmatrix} \tilde{\boldsymbol{f}}_{C_k} \\ \tilde{\boldsymbol{\mu}}_{C_k} \end{pmatrix} = \sum_j^{N_e} \begin{bmatrix} \boldsymbol{E}_3 \\ \$\left(\tilde{\boldsymbol{d}}_j\right) \end{bmatrix} \tilde{\boldsymbol{f}}_j = \boldsymbol{U}_k \boldsymbol{\beta}_k$$

where

$$\begin{aligned} \boldsymbol{U}_k &= \begin{bmatrix} \bar{\boldsymbol{U}}_1 & \cdots & \bar{\boldsymbol{U}}_{N_c} \\ \$\left(\tilde{\boldsymbol{d}}_1\right) \bar{\boldsymbol{U}}_1 & \cdots & \$\left(\tilde{\boldsymbol{d}}_{N_c}\right) \bar{\boldsymbol{U}}_{N_c} \end{bmatrix} \in \Re^{6 \times m N_c} \\ \boldsymbol{\beta}_k &= \begin{bmatrix} \boldsymbol{\alpha}_1 & \cdots & \boldsymbol{\alpha}_{N_c} \end{bmatrix}^T \Re^{m N_c} \end{aligned} \tag{8}$$

where $\bar{\boldsymbol{U}}_k$ is the basis matrix and $\tilde{\boldsymbol{d}}_j$ is the vector from $\{\mathcal{C}_k\}$ to each edge of the foot.

D. Control framework with task-space control

As described in (5), the control problem is to find the generalized coordinates acceleration and contact force to obtain the command torque $\boldsymbol{\tau}_C$

$$\boldsymbol{\tau}_C = \boldsymbol{M}_q \ddot{\boldsymbol{\xi}}^* + \boldsymbol{C}_q \dot{\boldsymbol{\xi}} + \boldsymbol{g}_q - \sum_k^{N_e} \boldsymbol{J}_{C_k}^T \boldsymbol{\lambda}_{C_k}^* \tag{9}$$

where $\ddot{\boldsymbol{\xi}}^*$, $\boldsymbol{\lambda}_{C_k}^*$ are obtained from optimization and the solution of QP satisfies the following tasks, constraints and objectives.

The problem in this paper has tasks: tracking CoM position & body orientation, tracking swing leg's trajectories, trunk orientation, and keeping contact constraints during support phase. As one of tasks, (3) is used for the swing foot.

By combining the tasks and constraints, we form the QP formulation:

$$\begin{aligned} \boldsymbol{z} = \min_{\ddot{\boldsymbol{\xi}}, \boldsymbol{\beta}_k} & ||\boldsymbol{M}_B \ddot{\boldsymbol{\xi}} - \boldsymbol{b}_1||_{W_1}^2 + \sum_t ||\boldsymbol{\Phi}_t \ddot{\boldsymbol{\xi}} - \boldsymbol{b}_t||_{W_t}^2 \\ & + ||\ddot{\boldsymbol{\xi}}||_{W_3}^2 + \sum_k ||\boldsymbol{\beta}_k||_{W_4}^2 \end{aligned}$$

subject to

$$\begin{aligned} \boldsymbol{M}_B \ddot{\boldsymbol{\xi}} + \boldsymbol{C}_B \dot{\boldsymbol{\xi}} + \boldsymbol{g}_B &= \sum_k^{N_e} \boldsymbol{X}_{C_k B}^T \tilde{\boldsymbol{R}}_{C_k} \boldsymbol{U}_k \boldsymbol{\beta}_k \\ \boldsymbol{\Phi}_t \ddot{\boldsymbol{\xi}} + \dot{\boldsymbol{\Phi}}_t \dot{\boldsymbol{\xi}} &= \boldsymbol{0} \qquad \text{(in support state)} \\ \boldsymbol{\Lambda}_k \boldsymbol{\beta}_k &\geq \boldsymbol{0} \end{aligned}$$

where

$$\begin{aligned} \boldsymbol{b}_1 &= \boldsymbol{X}_{GB}^T \dot{\boldsymbol{h}}_{G,r} - \boldsymbol{C}_B \dot{\boldsymbol{\xi}} \\ \boldsymbol{b}_t &= \ddot{\boldsymbol{x}}_r - \dot{\boldsymbol{\Phi}}_t \dot{\boldsymbol{\xi}} \end{aligned} \tag{10}$$

where $W_1, \cdots, W_4$ are objective function weighting matrices. In addition, task references become $\dot{\boldsymbol{h}}_{G,r} = \dot{\boldsymbol{h}}_{G,d} + \boldsymbol{K}_h \left(\boldsymbol{h}_{G,d} - \boldsymbol{h}_G\right) + \boldsymbol{K}_I \int \left(\boldsymbol{h}_{G,d} - \boldsymbol{h}_G\right) dt$ and $\ddot{\boldsymbol{x}}_r = \ddot{\boldsymbol{x}}_d + \boldsymbol{K}_V \left(\dot{\boldsymbol{x}}_d - \dot{\boldsymbol{x}}\right) + \boldsymbol{K}_P \left(\boldsymbol{x}_d - \boldsymbol{x}\right)$. $\ddot{\boldsymbol{x}}_r$ is the reference acceleration of tasks such as swing foot, arms, trunk. $\boldsymbol{x}, \boldsymbol{x}_d$ are current and the reference walking trajectory of the task. $\dot{\boldsymbol{x}}, \dot{\boldsymbol{x}}_d$ are the current and reference velocity of the swing foot. $\boldsymbol{\Phi}_t, \dot{\boldsymbol{\Phi}}_t$ are the task jacobian and it's derivative. These weighting matrices are determined for the walking motion. The QP is solved in every step of the control to satisfy the desired accelerations and the force intensities. Acceleration constraints are changed according to the leg's state.

IV. Simulation

As described in Fig. 1, the humanoid robot has 57 Kg of weight including 20 Kg for body, 10 Kg for each legs, and 6 Kg for each arms. It has 28 DoF with 22 joints (6 for each legs, 4 for each arms, 2 for trunk). The body motion $\dot{\boldsymbol{p}}_B, \boldsymbol{\omega}_B$ are known by the simulator. The simulation is performed using **MuJoCo** [25]. The control algorithms are programmed by C++ and simulation is performed with 2 KHz sampling rate including the control rate of 1 KHz.

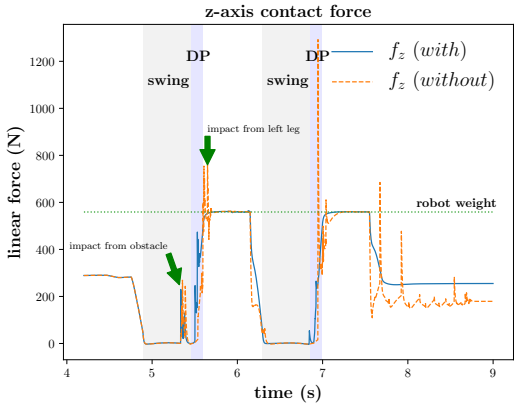

Fig. 4. Contact force comparison. Blue solid line is the contact force with the proposed algorithm and orange dashed line is the contact force without the algorithm. Green dotted line is the weight of the robot, shadowed area refers to the stance phase, and DP refers to double support phase.

Since most of the unexpected landing occurs in the z-axis position, x-axis & y-axis orientation, the simulation is performed with/without the proposed algorithm as a validation process. Every simulation in this paper has been run with the given x-direction walking pattern assumed with the plane ground, $0.35m$ of stride, $0.7s$ of one step ($0.56s$ for single support phase, $0.14s$ for double support phase). In addition, FT sensor has been mounted below the ankle so the movement of the robot leg generates small varied forces due to the foot dynamics. Hence, the force threshold hold is set as $10N$ for z-axis and $3Nm$ for x-axis & y-axis rotation axis. In addition, the modified values are initialized in the supporting state to avoid abusing by the integrator.

One primitive task and two hard constrained tasks are performed to compare the performance of the algorithm. The tasks are stepping on the obstacle. One is z-axis varied and two are tilted in x-axis and y-axis respectively. The obstacles are in the middle of right foot path. No information is given about the obstacle. The simulation has two steps. First is stepping on the obstacle and second is stepping down to the ground. In addition, complex task is given to overcome the uneven terrain with multiple obstacles consecutively in uploaded video.

A. Performance validation with and without the proposed algorithm

The obstacle with the height of $4cm$ can be overcome without the impedance control using the QP framework as described in section III. However, it is difficult to be overcome with the $5cm$ height obstacle. Hence, the impact force, energy consumption can be compared in $4cm$ height obstacle task.

Fig. 4. shows the contact forces with & without impedance control algorithm. Walking started from a double support state, and the right foot starts swinging from $4.892s$ to $5.592s$. In the swinging phase, the robot faced with the $4cm$ height obstacle at $5.33s$ and stepping on the obstacle. At the contact moment, the originally designed trajectory is

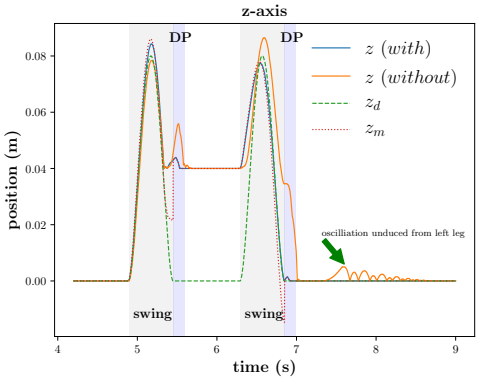

(a) z-axis position.

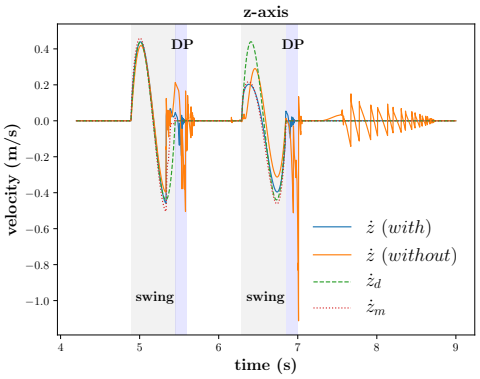

(b) z-axis linear velocity.

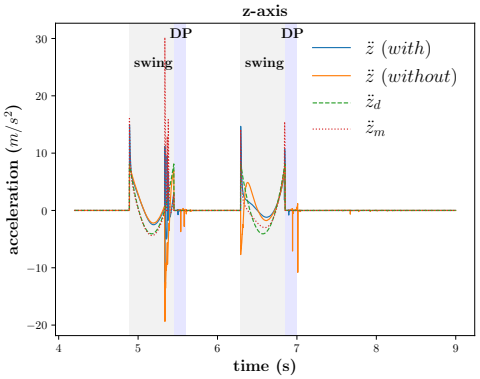

(c) z-axis linear acceleration.

Fig. 5. z-axis position, velocity, and acceleration. Blue and orange solid line is the current state value with and without the impedance control, the green dashed line is the originally given desired value, and red dotted line is the modified desired value by impedance control.

throughout the obstacle so the velocity sign is changed and high impact force is generated. In addition, the case also shows weakness to interference from the left leg. However, The robot with the proposed impedance control can overcome the unexpected force and smoothly step on the uneven terrain. It shows that the force from the left leg is reduced because the left leg also shows impedance behavior.

The Fig. 5 (a) shows the z-axis position. As described in I and II, tracking the desired trajectory after the contact makes undesirable force and motion, and it results in the break of stability. After contact, the impedance controller modifies the

desired trajectory and it generates less tracking error.

The Fig. 5 (b) shows the z-axis linear velocity of the right foot. When the contact occurs, the right foot tries to keep going down to track the designed trajectory and it makes oscillations so the landing becomes unstable as an orange dashed line. However, the impedance controller compensates for the oscillations so the velocity is regulated fast, and landing becomes complete.

The Fig. 5 (c) shows the z-axis acceleration. At the moment of contact, current state without impedance control has high peaks in negative direction because the errors of position and velocity make big acceleration to track the desired trajectory. Hence, The robot foot continuously hits the obstacle. In the case of the impedance control, the acceleration is generated in the direction of decreasing the velocity. It makes the robot landing stable.

The key idea of the proposed control is the generation of the proper reference input by modified position, velocity, acceleration altogether. Throughout, the performance of the proposed impedance control for humanoid locomotion has validated through the force and velocity figures.

B. Landing task on obstacle tilted by the x-axis & y-axis

As the performance of the impedance control is verified, a harder task is given to investigate the marginal bound of the controller. In the case without a proposed control algorithm, a small tilting angle ($< 1°$) with a $4cm$ height can be overcome. If the height of the obstacle is lowered as $3cm$, the tilting angle ($< 10°$) could be considered.

On the other hand, the obstacle with the height of $5cm$ and tilting angle by $20°$ has given for the proposed controller. It is difficult task because slip occurs easily so faster regulation of velocity is much important. As shown in Fig. 6, at the moment of contact, impulsive acceleration is generated however impedance controller modified to be compliant. Due to the modified acceleration, fluctuation of velocity is regulated fast so does the orientation.

Y-axis variation is also tested and similar results are obtained. In the case without the impedance control algorithm, phenomenon is quite similar to x-axis tilted case. A small tilting angle ($< 1°$) with a $4cm$ height can be overcome and the tilting angle ($< 9°$) could be considered with a $3cm$ height obstacle.

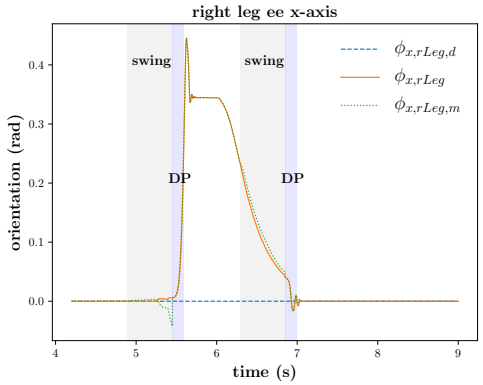

(a) x-axis orientation.

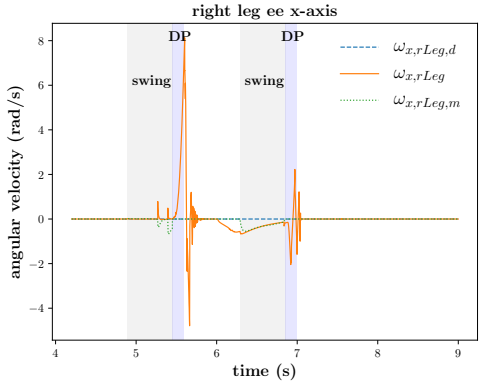

(b) x-axis angular velocity.

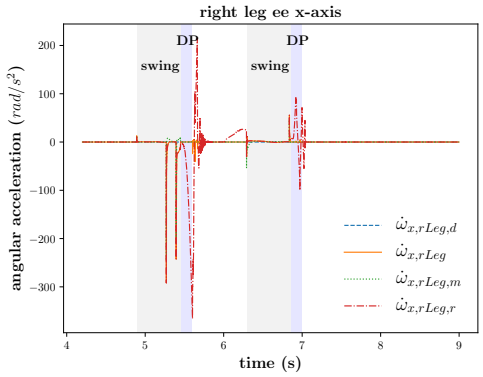

(c) x-axis angular acceleration.

Fig. 6. x-axis orientation, velocity, acceleration. Blue dotted line is the desired value, orange solid line is current state value, red dotted line is the modified desired value by the proposed controller.

V. Conclusion

This paper proposed impedance control based humanoid walking on uneven terrain, composed of the quadratic programming(QP) using centroidal dynamics. The proposed algorithm modify the desired position, velocity, and acceleration to get proper reference acceleration that is input of the QP framework to get the control torque. To investigate the performance of the controller, humanoid robot is simulated using Mujoco dynmaics engine. In the simulation, without the knowledge of the object, the performance of the proposed controller is compared with that of the torque control only with the QP framework. The impedance control framework with QP can walk tough uneven terrain without re-planning. Therefore, the controller shows better performance than the control only with QP framework.

Meanwhile, when the robot faced with a higher or more tilted terrain, slips in the direction of not considered in this paper occur. Hence, Those slips also will be handled with the proposed algorithm as future work.

References

[1] Y. Choi, D. Kim, Y. Oh, and B. You, "Posture/walking control for humanoid robot based on kinematic resolution of com jacobian with embedded motion," *IEEE Transactions on Robotics*, vol. 23, no. 6, pp. 1285–1293, Dec 2007.

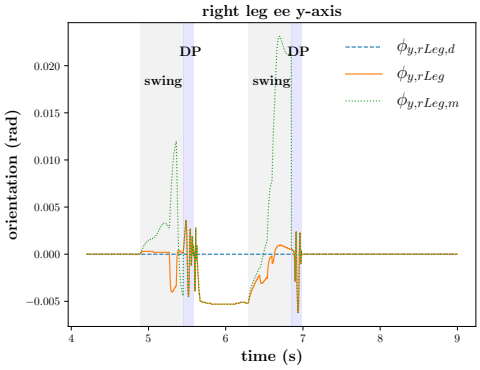

(a) y-axis orientation.

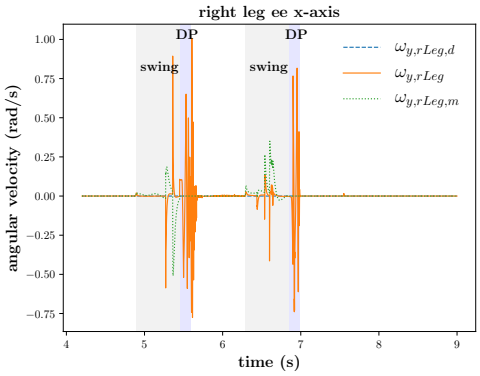

(b) y-axis angular velocity.

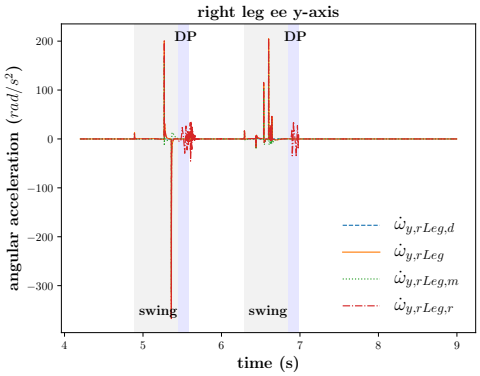

(c) y-axis angular acceleration.

Fig. 7. y-axis orientation, velocity, acceleration. Blue dotted line is the desired value, orange solid line is current state value, red dotted line is the modified desired value by the proposed controller.

[2] M. Mistry, J. Nakanishi, G. Cheng, and S. Schaal, "Inverse kinematics with floating base and constraints for full body humanoid robot control," in *Humanoids 2008 - 8th IEEE-RAS International Conference on Humanoid Robots*, Dec 2008, pp. 22–27.

[3] M. Mistry, J. Buchli, and S. Schaal, "Inverse dynamics control of floating base systems using orthogonal decomposition," in *2010 IEEE International Conference on Robotics and Automation*, May 2010, pp. 3406–3412.

[4] S. Hyon, J. G. Hale, and G. Cheng, "Full-body compliant human–humanoid interaction: Balancing in the presence of unknown external forces," *IEEE Transactions on Robotics*, vol. 23, no. 5, pp. 884–898, Oct 2007.

[5] L. Righetti, J. Buchli, M. Mistry, M. Kalakrishnan, and S. Schaal, "Optimal distribution of contact forces with inverse dynamics control," *International Journal of Robotics Research*, vol. 32, 03 2013.

[6] A. Herzog, N. Rotella, S. Mason, F. Grimminger, S. Schaal, and L. Righetti, "Momentum Control with Hierarchical Inverse Dynamics on a Torque-Controlled Humanoid," *arXiv e-prints*, p. arXiv:1410.7284, Oct 2015.

[7] S. Feng, E. Whitman, X. Xinjilefu, and C. G. Atkeson, "Optimization based full body control for the atlas robot," in *2014 IEEE-RAS International Conference on Humanoid Robots*, Nov 2014, pp. 120–127.

[8] S.-H. Lee and A. Goswami, "A momentum-based balance controller for humanoid robots on non-level and non-stationary ground," *Autonomous Robots*, vol. 33, no. 4, pp. 399–414, Nov 2012.

[9] T. Koolen, S. Bertrand, G. Thomas, T. De Boer, T. Wu, J. Smith, J. Englsberger, and J. Pratt, "Design of a momentum-based control framework and application to the humanoid robot atlas," *International Journal of Humanoid Robotics*, vol. 13, pp. 1 650 007–1, 03 2016.

[10] P. M. Wensing and D. E. Orin, "Improved computation of the humanoid centroidal dynamics and application for whole-body control," *International Journal of Humanoid Robotics*, vol. 13, no. 01, 2016.

[11] S. Kajita, M. Morisawa, K. Miura, S. Nakaoka, K. Harada, K. Kaneko, F. Kanehiro, and K. Yokoi, "Biped walking stabilization based on linear inverted pendulum tracking," in *2010 IEEE/RSJ International Conference on Intelligent Robots and Systems*. IEEE, 2010, pp. 4489–4496.

[12] I.-S. Kim, Y.-J. Han, and Y.-D. Hong, "Stability control for dynamic walking of bipedal robot with real-time capture point trajectory optimization," *Journal of Intelligent & Robotic Systems*, 2019.

[13] M. Kim, D. Lim, and J. Park, "Online walking pattern generation for humanoid robot with compliant motion control," *Proceedings - IEEE International Conference on Robotics and Automation*.

[14] J. Ding, Y. Wang, M. Yang, and X. Xiao, "Walking stabilization control for humanoid robots on unknown slope based on walking sequences adjustment," *Journal of Intelligent & Robotic Systems*, vol. 90, no. 3, pp. 323–338, Jun 2018.

[15] J.-Y. Kim, I.-W. Park, and J.-H. Oh, "Walking control algorithm of biped humanoid robot on uneven and inclined floor," *Journal of Intelligent and Robotic Systems*, vol. 48, pp. 457–484, 2007.

[16] S. M. Yoo, S. W. Hwang, D. H. Kim, and J. H. Park, "Biped robot walking on uneven terrain using impedance control and terrain recognition algorithm," in *2018 IEEE-RAS 18th International Conference on Humanoid Robots (Humanoids)*. IEEE, 2018, pp. 293–298.

[17] W. Xu, R. Xiong, and J. Wu, "Force/torque-based compliance control for humanoid robot to compensate the landing impact force," in *2010 First International Conference on Networking and Distributed Computing*, Oct 2010, pp. 336–340.

[18] Y. Kim, B. Lee, J. Ryu, and J. Kim, "Landing force control for humanoid robot by time-domain passivity approach," *IEEE Transactions on Robotics*, vol. 23, no. 6, Dec 2007.

[19] Y. Kim, I. Park, J. Yoo, and J. Kim, "Stabilization control for humanoid robot to walk on inclined plane," in *Humanoids 2008 - 8th IEEE-RAS International Conference on Humanoid Robots*, Dec 2008, pp. 28–33.

[20] Jong Hyeon Park and Hoam Chung, "Hybrid control for biped robots using impedance control and computed-torque control," in *Proceedings 1999 IEEE International Conference on Robotics and Automation (Cat. No.99CH36288C)*, vol. 2, 1999, pp. 1365–1370 vol.2.

[21] J. Park and J. H. Park, "Impedance control of quadruped robot and its impedance characteristic modulation for trotting on irregular terrain," in *2012 IEEE/RSJ International Conference on Intelligent Robots and Systems*, Oct 2012, pp. 175–180.

[22] B. G. Son, J. T. Kim, and J. H. Park, "Impedance control for biped robot walking on uneven terrain," in *2009 IEEE International Conference on Robotics and Biomimetics (ROBIO)*, Dec 2009, pp. 239–244.

[23] S. Hong, Y. Oh, D. Kim, and B. You, "A walking pattern generation method with feedback and feedforward control for humanoid robots," in *2009 IEEE/RSJ International Conference on Intelligent Robots and Systems*, 2009, pp. 1078–1083.

[24] M. Nikolić, B. Borovac, and M. Raković, "Dynamic balance preservation and prevention of sliding for humanoid robots in the presence of multiple spatial contacts," *Multibody System Dynamics*, vol. 42, no. 2, pp. 197–218, Feb 2018.

[25] E. Todorov, T. Erez, and Y. Tassa, "Mujoco: A physics engine for model-based control," in *2012 IEEE/RSJ International Conference on Intelligent Robots and Systems*, 2012, pp. 5026–5033.